Proximity effect in $YBa_2Cu_3O_{7-y}/PrBa_2Cu_3O_{7-y}$ superlattices studied by inelastic light scattering

D. Budelmann, S. Ostertun, M. Rübhausen, A. Bock, M. Schilling, H. Burkhardt, and U. Merkt
Institut für Angewandte Physik und Zentrum für Mikrostrukturforschung, Universität Hamburg, Jungiusstraße 11, D-20355 Hamburg, Germany

A. Krämer
Technische Universität Hamburg-Harburg, Abteilung Mikrosystemtechnik, Eißendorfer Straße 42, D-21073 Hamburg, Germany

(Received 15 September 2000; published 9 April 2001)

We have employed inelastic light scattering of phonons in $YBa_2Cu_3O_{7-y}/PrBa_2Cu_3O_{7-y}$ superlattices to study proximity-induced phonon self-energy effects. The $PrBa_2Cu_3O_{7-y}$ (PBCO) oxygen out-of-phase vibrations in the CuO_2 layer show a typical hardening of about 3 cm^{-1} and a narrowing of about 1 cm^{-1} below the critical temperature T_c of the superlattice. These are absent in pure PBCO samples, demonstrating that the proximity effect occurs homogeneously in the insulating barrier and that the proximity-induced Cooper pairs exhibit an energy gap $2\Delta_{PBCO}$ which is much smaller than the PBCO out-of-phase phonon frequency.

DOI: 10.1103/PhysRevB.63.174508 PACS number(s): 74.25.Bt, 63.20.Kr, 78.30.−j, 74.50.+r

I. INTRODUCTION

Transport between high-T_c superconductors (HTC's) through insulating and nonsuperconducting barriers has attracted a lot of attention.[1–3] Especially, the observation of a so-called ''long-range'' proximity (LRP) effect has provided various proposed conduction mechanisms through the insulating barriers, i.e., resonant tunneling, tunneling via multiple localized states, and variable-range hopping.[4] Whether the LRP effect is due to Josephson coupling or filamentary superconducting channels is not yet known.[5] Moreover, it is unclear whether the LRP effect occurs homogeneously in the insulating barrier and whether the conventional proximity effect plays a significant role.[6,7]

Unfortunately, many otherwise very useful experimental techniques like angle-resolved photon emission spectroscopy and neutron scattering are not available to study the proximity effect in multilayer compounds. Inelastic light scattering (ILS) has provided a rich variety of information on charge, spin, and lattice degrees of freedom in cuprate superconductors.[8–15,18,19] Superconductivity leaves its signature in the ILS spectra through one or several of the following phenomena: (a) There is an opening of the superconducting gap redistributing the electronic background.[8–12] However, the gap is strongly doping dependent and the gap signatures weaken for underdoped samples.[11–13] (b) Phonon self-energy effects result in anomalous softening or hardening in the phonon frequencies for gap values above or below the phonon frequency, respectively.[14–17] (c) At higher energies a redistribution of spectral weight which is related to the magnetic degrees of freedom is observed.[18,19]

Inelastic light scattering on different $YBa_2Cu_3O_{7-y}/PrBa_2Cu_3O_{7-y}$ (YBCO/PBCO) superlattices has been performed by several groups discussing mostly Brillouin-zone-folding effects.[20–22] So far, no conclusive superconductivity-induced effects on the PBCO phonons have been found. However, Litvinchuk *et al.* have observed a hardening but no narrowing of the PBCO oxygen out-of-phase vibration O(2)-O(3) or B_{1g} mode in the CuO_2 double layer below 100 K. They have attributed this effect to the anharmonic decay.[20]

Here we demonstrate that the proximity effect in YBCO/PBCO superlattices can be studied by ILS through the superconductivity-induced hardening and narrowing of the PBCO O(2)-O(3) vibration, which is absent in similarly manufactured PBCO films. Since ILS is a local volume probe, we conclude that the proximity effect in PBCO is indeed an intrinsic property. The fact that the YBCO phonon softens and the PBCO phonon hardens indicates that the superconducting gap in YBCO is significantly larger than the gap of the proximity-induced Cooper pairs in PBCO. Based on a simple estimate from our Raman data, we suggest a relation between the gap magnitudes of $2\Delta_{YBCO} > \hbar\omega_{YBCO}^{O(2)\text{-}O(3)} > \hbar\omega_{PBCO}^{O(2)\text{-}O(3)} > 2\Delta_{PBCO}$.

II. EXPERIMENT

We have used pulsed laser deposition (PLD) with a multiple target holder for the fabrication of the *c*-axis-oriented superlattices and the reference YBCO and PBCO films on $SrTiO_3$ (STO) (100) substrates.[23] Growth of the superlattice was achieved on planar surfaces and ramps. The investigation of ramps compared to planar surfaces should allow one to examine the impact of the a/b-axis coupling onto the *c*-axis coupling. Several ramps with various angles and widths were etched by argon-ion milling into the substrates.[24] Second, deposition using an excimer KrF laser took place at a substrate temperature of 1090 K, a laser wavelength of 248 nm, a laser energy density of 2 J/cm^2, a laser repetition rate of 3 Hz, and an oxygen pressure of 3 Pa. The deposition rates have been determined by an atomic-force microscope (AFM). After deposition of one initial YBCO layer with a thickness of 60 nm to promote *c*-axis growth, to reduce substrate strain, and to block scattering signals of the substrate, alternating layers of PBCO and YBCO with layer thicknesses of 4:4 (R752) and 6:6 (R750)

 ©2001 The American Physical Society

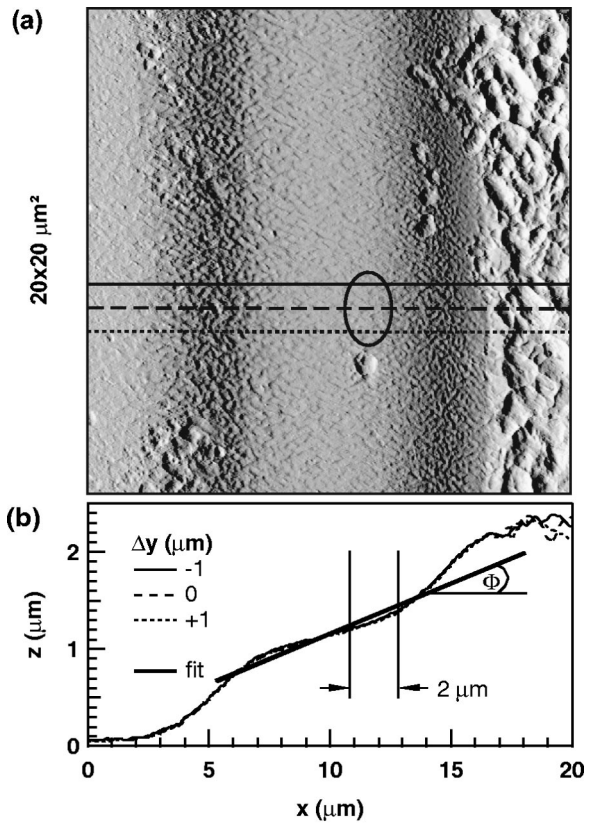

FIG. 1. (a) Typical ramp on sample R752 characterized by atomic-force microscopy on an area of $20\times20\ \mu m^2$. (b) The different curves correspond to the line measurements as shown in (a). They are virtually identical, outlining the lateral homogeneity of the ramp. The spot diameter of the light is about $3\times2\ \mu m^2$ as indicated. The fit is used to determine the ramp angle Φ.

unit cells were grown, respectively. The PBCO and YBCO layers were deposited 27 times for sample R752 and 18 times for R750, yielding a total film thickness of about 300 nm. In the following, measurement locations above or below the ramps are named planar. Superlattice constants of 8.82 and 13.36 nm were determined from the satellite peaks found next to the $(00l)$ x-ray diffraction peaks of YBCO and PBCO.

The sample surfaces have been bonded with indium to perform standard four-terminal resistance measurements in van der Pauw geometry. Zero-resistance temperatures T_c and transition widths ΔT_c (10–90 %) of the YBCO/PBCO superlattices and the YBCO film have been obtained. For the superlattices we have found $T_c=(82.0\pm1.9)$K with $\Delta T_c=2.8$ K and $T_c=(79.8\pm2.3)$K with $\Delta T_c=3.6$ K for the samples R752 and R750, respectively. The YBCO film has exhibited zero resistance at $T_c=(82.2\pm1.4)$K with $\Delta T_c=2.8$ K, whereas the PBCO film has shown no superconducting, but typical semiconducting behavior for the entire temperature range. This is contrary to some PBCO samples exhibiting superconducting properties under certain conditions.[25]

Topology and surface morphology of the superlattices have been determined by AFM. As shown in Fig. 1(a), we find increased roughness due to droplets and outgrowths on the upper side of the ramp (right side) caused by redeposited STO particles during the argon-ion milling. Ramp heights of about 2.5 μm and angles from 4° to 6° have been obtained. The effective widths of the studied ramps have been measured to vary between 8 and 12 μm. The line measurements plotted in Fig. 1(b) are typical for all ramps. They show the lateral homogeneity of the ramp along the y direction. Outgrowths and droplets helped to map the ramp angle exactly to the location of the corresponding ILS measurement. We observe crystalline growth on the ramps with a typical rms roughness of about 5 nm on an area of 25 μm^2, whereas the planar sample surfaces are smoother with 2.5 nm rms roughness. The thickness d_c of the PBCO barrier perpendicular to the *ab* plane is given by half of the superlattice constant, whereas the barrier thickness parallel to the copper planes has been estimated by the relation $d_{ab}=d_c/\tan\Phi$, with Φ being the ramp angle.

Raman spectra of the YBCO/PBCO superlattices and the reference films have been taken at various sample temperatures between 10 and 290 K in backscattering configuration, analyzed by a triple-grating spectrometer, and detected with a LN_2-cooled charge-coupled device camera. The spectra have been calibrated to the spectrometer sensitivity using a double Ulbricht sphere system and divided by the thermal Bose factor $[1+n(\omega)]$ as described elsewhere.[18] For the measurements we have used the 514.5-nm line of an argon-ion laser. The beam was focused on the *ab*-plane sample surface as sketched in Fig. 1(a) to a spot diameter of $3\times2\ \mu m^2$ that includes 80% of the power. We employed an incident power of 0.4 mW to limit local heating to temperatures of about 5 K. The scattered signal was collected using a 50× ultralong working distance objective with correction for the cryostat window.

All ILS measurements on the superlattices and different locations on the planar surfaces lead to spectra exhibiting separated PBCO and YBCO phonon modes. The absence of mixed modes, which would be typical for $Y_{1-x}Pr_xBa_2Cu_3O_7$, indicates well-defined interfaces and an insignificant Y/Pr-ion interdiffusion.[27] In the following, we focus on the O(2)-O(3) modes obtained in depolarized B_{1g} symmetry, which have energies near the superconducting gap. Raman spectra obtained below T_c did not show an electronic background with a superconducting energy gap. This behavior is known from the underdoped regime of the samples with $y>0.15$ and corresponds well to the slightly reduced transition temperatures.[15]

III. RESULTS AND DISCUSSION

Raman spectra of the superlattice R750 measured on a ramp and a planar surface are shown in Fig. 2. The superposition of the well-known O(2)-O(3) vibrations belonging to PBCO and YBCO can be found at about 300 and 340 cm^{-1}, respectively.[26,27] In order to describe the spectra, a Lorentzian profile has been employed to represent the PBCO phonon, whereas the YBCO phonon has been fitted to a Fano line shape

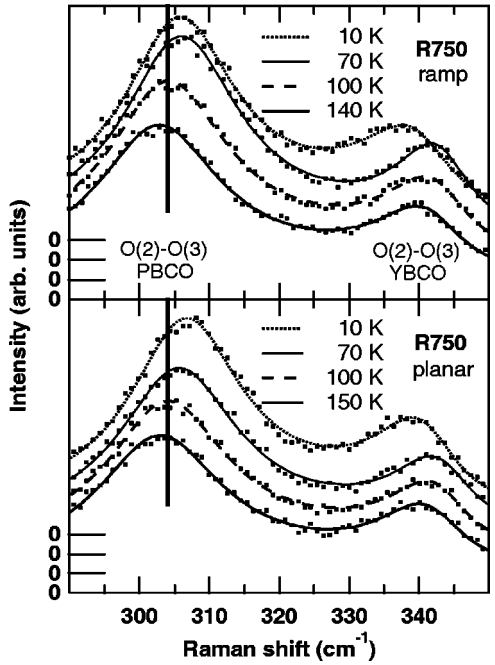

FIG. 2. B_{1g} spectra of the superlattice R750 at several temperatures. The lines represent fits to the phonons and the background. The PBCO phonon frequencies $\omega_{0,N} \simeq 304\,\mathrm{cm}^{-1}$ (bold vertical lines) are obtained by a fit of the data for $T > T_c$ to an anharmonic decay (see text). The PBCO phonons show an additional hardening below T_c, whereas the 340-cm^{-1} YBCO mode softens on the ramp and planar surface.

$$I_{\mathrm{Fano}}(\omega) \propto \frac{(\epsilon+q)^2}{1+\epsilon^2}, \tag{1}$$

where $\epsilon = (\omega - \omega_\nu)/\gamma$. The Fano parameter q describes the asymmetry of the line shape and the strength of the phonon coupling to the electronic continuum. The phonon frequency and linewidth [half width at half maximum (HWHM)] are given by ω_ν and γ, respectively. An expression that is often used to model the electronic response of the normal state in the cuprates is given by

$$I_{\mathrm{bg}}(\omega) \propto \tanh(\omega/\omega_T), \tag{2}$$

where the thermal crossover frequency ω_T describes the transition of the background from a linear to a constant behavior.[12,28] Equation (2) characterizes the typical inelastic scattering rate leading to an incoherent background within the marginal and nested Fermi-liquid theories. From this fit and by inspecting Fig. 2, we estimate the additional hardening below T_c of the PBCO O(2)-O(3) vibration to be up to 3 cm^{-1}.

Figure 3 shows the temperature dependence of the phonon frequencies for the reference films and the superlattice R752. The B_{1g} mode of the PBCO film is compared to the phonon measured on the ramp of R752 in Fig. 3(b). The critical temperature T_c of the superlattice is represented by the dashed vertical line. The anharmonic decay for phonons with a wave vector $\mathbf{q}=0$ as indicated by the solid lines in Figs. 3–5 is given by

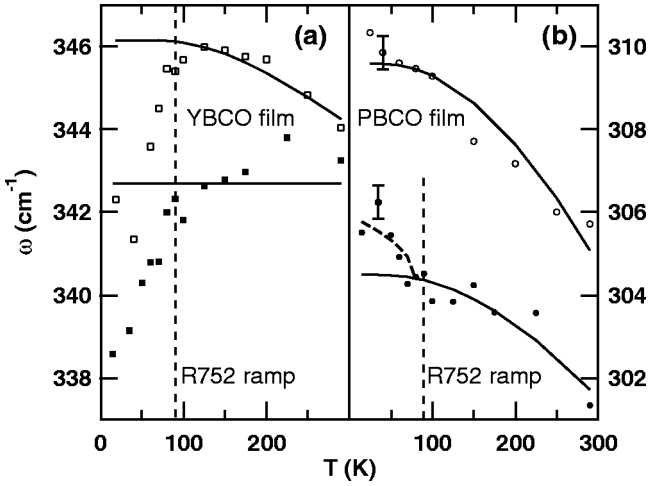

FIG. 3. Temperature dependence of the B_{1g} phonon frequencies for (a) pure YBCO and (b) PBCO films (open symbols) and the superlattice R752 (solid symbols). Vertical dashed lines indicate T_c. Anharmonic decay is shown by solid lines. The proximity-induced hardening below T_c is represented by the dashed curve. The PBCO film shows no superconductivity-induced effects.

$$\omega(T) = \omega_0 - A\Delta_1(\omega_0, T) - B\Delta_2(\omega_0, T), \tag{3}$$

where the decay to two phonons is represented by

$$\Delta_1(\omega_0, T) = 1 + 2[\exp(\hbar\omega_0/2k_BT) - 1]^{-1} \tag{4}$$

and the decay to three phonons by

$$\Delta_2(\omega_0, T) = 1 + 3[\exp(\hbar\omega_0/3k_BT) - 1]^{-1} + 3[\exp(\hbar\omega_0/3k_BT) - 1]^{-2}, \tag{5}$$

with the phonon frequency ω_0 at $T=0$. Here A and B are the cubic and quartic matrix elements of the respective decay channel.[29,30] The temperature dependence is well modeled by Eq. 3 for $T > T_c$. All curves are described by parameters $A \ll 1\,\mathrm{cm}^{-1}$ and $B \approx 1\,\mathrm{cm}^{-1}$, indicating that the quartic term is preferred. This agrees with the result documented in the literature.[30] The $T=0$ phonon frequency $\omega_{0,N} := \omega_0 - A - B$ takes anharmonic decay into account. Below T_c, an additional shift $\Delta\omega$ from $\omega_{0,N}$ to higher frequencies has been found for the PBCO phonon of the superlattices, but not for the reference PBCO film. These phonon self-energy effects have been studied intensively in literature and are due to a change of the interaction between phonons and electrons induced by the formation of Cooper pairs.[14–17] Phonons with an energy larger than the superconducting energy gap are repelled and phonons with an energy smaller than the gap are attracted to it. Hence we attribute this additional hardening to be induced by superconductivity, as also occurs below T_c of the superlattice. Figure 3(a) shows the corresponding B_{1g} phonon in YBCO compared to the vibration in the YBCO film. Anharmonic decay could not be fitted properly using Eq. (3) as indicated by the constant solid line with $A=B=0$. Even though no gap structure has been found in the electronic background of the raw spectra, we can use the frequency shifts as indicators for the energy gaps. The two observed phonon effects let us conclude on the existence of

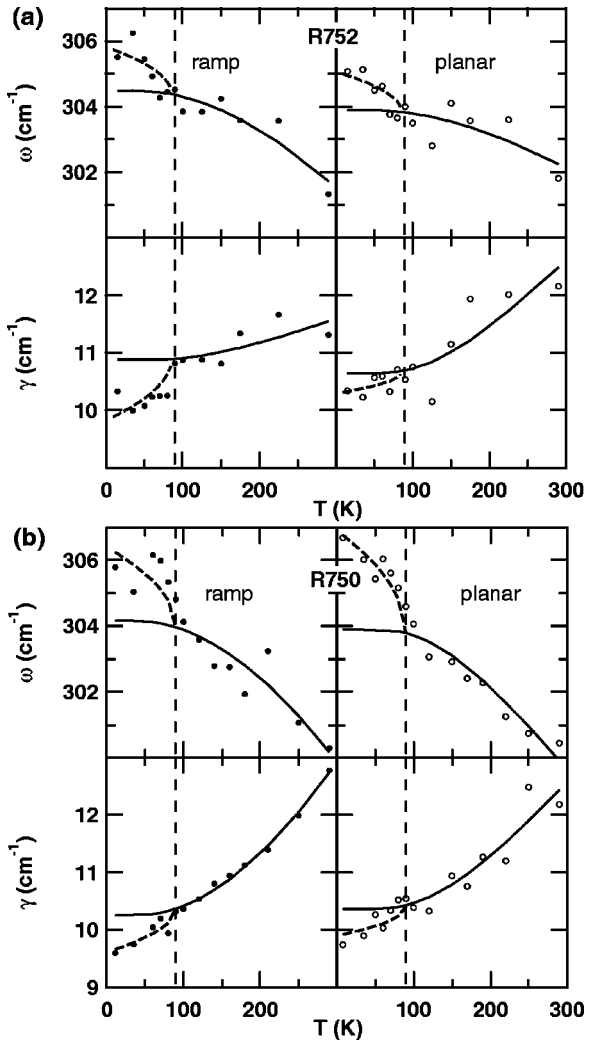

FIG. 4. Temperature-dependent phonon frequencies and linewidths (HWHM) of the O(2)-O(3) PBCO mode for (a) R752 and (b) R750. Similar behavior is found for each superlattice on ramps and planar locations. Vertical dashed lines indicate T_c. Proximity-induced hardening and sharpening are represented by dashed curves below T_c.

two gaps below T_c. The first gap $2\Delta_{\mathrm{YBCO}}$ couples to the YBCO phonon. It is larger than the phonon energy and forces the phonon to soften. The second gap induced by Cooper pairs tunneling through the PBCO layers, $2\Delta_{\mathrm{PBCO}}$, couples to the PBCO phonon, causing this phonon to harden. Therefore, the energy of this gap must be lower than the energy of the phonon and, accordingly, $2\Delta_{\mathrm{YBCO}} > \hbar\omega_{\mathrm{YBCO}}^{\mathrm{O(2)\text{-}O(3)}} > \hbar\omega_{\mathrm{PBCO}}^{\mathrm{O(2)\text{-}O(3)}} > 2\Delta_{\mathrm{PBCO}}$.

The temperature dependences of frequencies and linewidths measured on different locations of the superlattices are shown in Fig. 4. As a first approach to describe the hardening of the PBCO phonon frequency for $T<T_c$, we use an empirical phase transition formula

$$\omega(T)=\Delta\omega\sqrt{1-T/T_c}+\omega_{0,N}, \tag{6}$$

with $\Delta\omega$ being the frequency shift. Negative and positive shifts $\Delta\omega$ indicate softening and hardening of the phonon, respectively. The hardening of the PBCO phonon is observed in all measurements. We could not see any significant difference of the effects when comparing results for ramps or planar surfaces. Interplanar coupling between YBCO and PBCO CuO_2 planes through a barrier with thickness d_{ab}, as found on the ramps, does not seem to affect the B_{1g} modes especially. However, the existence of a strong proximity effect in the PBCO layers makes it rather unlikely that the hardening is just the result of the remaining Cooper pair amplitude in PBCO. This suggests that the unconventional behavior of PBCO gives rise to an intrinsic contribution, i.e., enhanced pairing or delocalization of holes bound to Pr.[25,27]

Anharmonic decay of the phonon linewidths has been fitted with an expression

$$\gamma(T)=\gamma_0+C\Delta_1(\omega_0,T)+D\Delta_2(\omega_0,T), \tag{7}$$

similar to Eq. (3) with constants C and D.[30] We have determined the linewidth shift $\Delta\gamma$ in analogy to Eq. (6). As shown in Fig. 4, the linewidth of the PBCO phonons follows the anharmonic decay for $T>T_c$. Below T_c, it sharpens, indicating most likely a reduced scattering of the phonons from impurities for $T<T_c$.

As listed in Table I we find that the superconductivity-induced hardening of the PBCO modes for the R750 superlattice is larger than for R752, while we would have expected an enhanced effect for the smaller barrier thickness d_c. To explain this behavior, we suggest impurity scattering in R752, resulting in an increased sharpening of the corresponding linewidth and a reduction of the hardening effect. This sharpening is consistent with observations on bulk materials by other groups.[15] Alternatively, we cannot exclude sample roughness having a larger impact on R752.

TABLE I. Shifts of frequency $\Delta\omega$ and linewidth $\Delta\gamma$ in cm^{-1}. Barrier thicknesses perpendicular, d_c, and parallel to the ab plane, d_{ab}, are given in nm.

	O(2)-O(3) PBCO		O(2)-O(3) YBCO		Barrier thickness	
Location	$\Delta\omega$	$\Delta\gamma$	$\Delta\omega$	$\Delta\gamma$	d_c	d_{ab}
R752 ramp	+1.5	−1.1	−4.0	+0.6	4.41	43.1
R752 planar	+1.2	−0.4	−4.1	+0.6	4.41	
R750 ramp	+2.4	−0.7	−2.6	+1.3	6.68	136.6
R750 planar	+3.1	−0.5	−1.3	+1.2	6.68	
YBCO film			−4.5	+1.7		

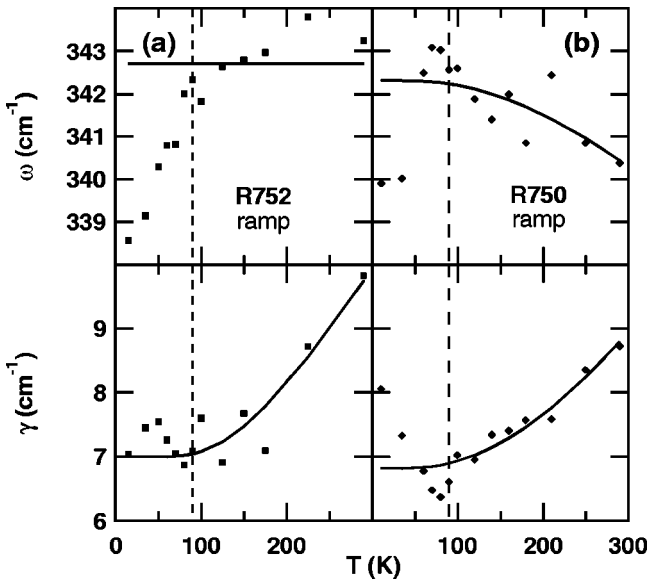

FIG. 5. Phonon frequencies and linewidths of the O(2)-O(3) YBCO mode vs temperature on ramps (a) R752 and (b) R750. Anharmonic decays are represented by the solid lines. The results on the planar surfaces exhibit similar properties.

The frequency and linewidth of the YBCO phonons measured on the ramps are depicted in Fig. 5. The temperature dependence is typical for each sample, but independent of the location of the laser spot on the ramp or planar surface of the respective sample. The superlattices provide different linewidth broadenings of the YBCO phonon. It is found to be enhanced for R750 compared to R752, supporting the suggestion of enhanced damping effects in R752 as caused by impurity scattering or interface artifacts.

IV. CONCLUSIONS

By comparing different YBCO/PBCO *c*-axis superlattices with YBCO and PBCO reference films, we demonstrate that the proximity effect in the YBCO/PBCO superlattices leaves its signature in the ILS spectra through a hardening and narrowing of the O(2)-O(3) PBCO phonon. This result outlines that this proximity effect is homogeneous within the PBCO layer of the superlattice. It is not a local artifact, and ILS is indeed a valuable technique to study local volume properties in nanometer-sized heterostructures.

Moreover, we show that this proximity effect is observed in superlattices of different periodicity and on ramped surfaces, although the interface morphology varies significantly. Finally, we suggest a relation between the gap values of $2\Delta_{\mathrm{YBCO}} > \hbar\omega_{\mathrm{YBCO}}^{\mathrm{O(2)\text{-}O(3)}} > \hbar\omega_{\mathrm{PBCO}}^{\mathrm{O(2)\text{-}O(3)}} > 2\Delta_{\mathrm{PBCO}}$.

ACKNOWLEDGMENTS

We thank M. Karger for the x-ray diffraction measurements, G. Meier for the introduction to atomic-force microscopy, and J. Müller for making his preparational facilities available to us. Financial support from the Deutsche Forschungsgemeinschaft via the Graduiertenkolleg ''Physik nanostrukturierter Festkörper,'' Sonderforschungsbereich 508 ''Quantenmaterialien,'' and Contract No. Ru773/2-1 is gratefully acknowledged.

[1] K. A. Delin and A. W. Kleinsasser, Supercond. Sci. Technol. **9**, 227 (1996).
[2] E. Polturak, G. Koren, D. Cohen, E. Aharoni, and G. Deutscher, Phys. Rev. Lett. **67**, 3038 (1991).
[3] A. M. Cucolo, R. Di Leo, A. Nigro, P. Romano, F. Bobba, E. Bacca, and P. Prieto, Phys. Rev. Lett. **76**, 1920 (1996).
[4] U. Kabasawa, Y. Tarutani, M. Okamoto, T. Fukazawa, A. Tsukamoto, M. Hiratani, and K. Takagi, Phys. Rev. Lett. **70**, 1700 (1993).
[5] B. H. Moeckly, D. K. Lathrop, and R. A. Buhrman, Phys. Rev. B **47**, 400 (1993).
[6] J. Z. Wu, X. X. Yao, C. S. Ting, and W. K. Chu, Phys. Rev. B **46**, 14 059 (1992).
[7] H. Zhao, J.-L. Shen, and Z. X. Zhao, Physica C **333**, 242 (2000).
[8] S. L. Cooper, M. V. Klein, B. G. Pazol, J. P. Rice, and D. M. Ginsberg, Phys. Rev. B **37**, 5920 (1988).
[9] R. Hackl, W. Gläser, P. Müller, D. Einzel, and K. Andres, Phys. Rev. B **38**, 7133 (1988).
[10] A. Yamanaka, T. Kimura, F. Minami, K. Inoue, and S. Takekawa, Jpn. J. Appl. Phys., Part 2 **27**, L1902 (1988).
[11] A. Bock, Ann. Phys. (Leipzig) **8**, 441 (1999).
[12] A. Bock, S. Ostertun, R. Das Sharma, M. Rübhausen, K.-O. Subke, and C. T. Rieck, Phys. Rev. B **60**, 3532 (1999).
[13] M. Opel, R. Nemetschek, C. Hoffmann, R. Philipp, P. F. Müller, R. Hackl, I. Tüttö, A. Erb, B. Revaz, E. Walker, H. Berger, and L. Forró, Phys. Rev. B **61**, 9752 (2000).
[14] B. Friedl, C. Thomsen, and M. Cardona, Phys. Rev. Lett. **65**, 915 (1990).
[15] E. Altendorf, X. K. Chen, J. C. Irwin, R. Liang, and W. N. Hardy, Phys. Rev. B **47**, 8140 (1993).
[16] E. J. Nicol, C. Jiang, and J. P. Carbotte, Phys. Rev. B **47**, 8131 (1993).
[17] R. Zeyher and G. Zwicknagel, Z. Phys. B: Condens. Matter **78**, 175 (1990).
[18] M. Rübhausen, C. T. Rieck, N. Dieckmann, K.-O. Subke, A. Bock, and U. Merkt, Phys. Rev. B **56**, 14 797 (1997).
[19] S. Sugai and T. Hosokawa, Phys. Rev. Lett. **85**, 1112 (2000).
[20] A. P. Litvinchuk, C. Thomsen, I. E. Trofimov, H.-U. Habermeier, and M. Cardona, Phys. Rev. B **46**, 14 017 (1992).
[21] K.-M. Ham, R. Sooryakumar, C. Kwon, Q. Li, and T. Venkatesan, Phys. Rev. B **48**, 16 744 (1993).
[22] R. Li, R. Feile, T. Hahn, G. Jakob, and H. Adrian, Phys. Rev. B **51**, 1322 (1995).
[23] J.-K. Heinsohn, D. Reimer, A. Richter, K.-O. Subke, and M. Schilling, Physica C **299**, 99 (1998).
[24] C. Francke, L. Mex, A. Krämer, and J. Müller, IEEE Trans. Appl. Supercond. **7**, 2768 (1997).
[25] Z. Zou, J. Ye, K. Oka, and Y. Nishihara, Phys. Rev. Lett. **80**, 1074 (1998).

[26] G. Burns, F. H. Dacol, C. Feild, and F. Holtzberg, Physica C **181**, 37 (1991).
[27] W. Widder, M. Stebani, L. Bauernfeind, H. F. Braun, K. Widder, H. P. Geserich, M. Rübhausen, N. Dieckmann, and A. Bock, Physica C **256**, 168 (1996).
[28] A. Virosztek and J. Ruvalds, Phys. Rev. B **45**, 347 (1992).
[29] M. Balkanski, R. F. Wallis, and E. Haro, Phys. Rev. B **28**, 1928 (1983).
[30] D. Mihailovic, K. F. McCarty, and D. S. Ginley, Phys. Rev. B **47**, 8910 (1993).